High-sensitivity temperature sensor based on Bragg grating in BDK-doped photosensitive polymer optical fiber

Xusheng Cheng (程旭升)[1], Weiwei Qiu (邱薇薇)[1], Wenxuan Wu (武文轩)[2], Yanhua Luo (罗艳华)[2], Xiujie Tian (田秀杰)[2], Qijin Zhang (张其锦)[2], and Bing Zhu (朱 冰)[1*]

[1]*Department of Electronic Engineering and Information Science, University of Science and Technology of China, Hefei 230026, China*

[2]*Anhui Key Laboratory of Soft Matter Chemistry, Department of Polymer Science and Engineering, University of Science and Technology of China, Hefei 230026, China*

*Corresponding author: zbing@ustc.edu.cn

A single-mode polymer optical fiber (POF) with highly photosensitive core doped with benzil dimethyl ketal (BDK) is fabricated and used for writing Bragg grating through the two-beam interference method. The Bragg wavelength of the grating is about 1570 nm, while the full-width at half-maximum (FWHM) of the reflection peak is 0.3 nm. The temperature response of POF Bragg grating is theoretically analyzed and experimentally measured in contrast to silica optical fiber Bragg grating (FBG). The result shows that the temperature character of POF Bragg grating is negative, which is opposite to the silica optical FBG. The absolute value of the temperature response of POF Bragg grating is one order of magnitude higher than that of the silica optical FBG, making POF Bragg grating appear to be very attractive for constructing temperature sensors with high resolution.

OCIS codes: 060.3738, 060.2370, 060.3735.

doi: 10.3788/COL201109.020602.

Optical fiber Bragg grating (FBG) sensors have attracted substantial interests in recent years and are well known for their capabilities for measuring many physical aspects. Compared with conventional electrical sensors, optical FBG sensors can offer important advantages such as electromagnetic interference (EMI) immunity, high sensitivity, and distributed sensing[1]. Most gratings are written in silica optical fibers and have been well developed and used as sensors of temperature[2], strain[3], pressure[4], bending[5,6], and refractive index[7], among others. However, the Bragg wavelength of the grating can only shift in a narrow range due to the physical character of the silica material, which limits the resolution of the sensor and makes the detecting devices very costly. On the contrary, the polymer material has bigger thermo-optic, thermal expansion, and electro-optic coefficients, which are several orders of magnitude higher than silica. Some significant studies on using polymer material to increase the sensitivity of the sensor have been carried out, such as using polymer packaging[8,9] and evanescent field coupling with polymer planar waveguide[10]. Since the first report of polymer optical fiber (POF) Bragg grating in 1999[11], an increasing number of research activities have been done about POF grating, and different kinds of POF grating have been fabricated[12−14]. The POF has many advantages; it is very cheap, rugged, and easy to connect. The drawing process of POF is at low temperature, thus rare-earth ion and organic chromophores can be doped into the POF without being destroyed[15]. The sensitivities of these sensors using Bragg grating writing in POF can be up to 10 times bigger than those of silica optical fiber[16]. However, there are still various problems, such as small refractive index change, long exposure time, and specified writing light wavelength, in the fabricated process. Different materials are commonly doped into the core of POFs to obtain high photosensitivity.

In this letter, we fabricate POF with a photosensitive core doped with benzil dimethyl ketal (BDK) and use it for writing FBG. To our knowledge, it is the first report that inscribes Bragg grating on the POF with a BDK-doped sensitive core used as temperature sensor. The POF is operated in single mode. The Bragg wavelength of the fiber grating in the POF is measured at around 1570 nm at room temperature (20 °C). The temperature response character of the polymer FBG is theoretically analyzed and experimentally verified. Experimental results are in good agreement with the theoretical analysis.

The Bragg wavelength of a FBG is given as[17]

$$\lambda_{\mathrm{B}} = 2n_{\mathrm{eff}}\Lambda, \tag{1}$$

where Λ is the grating period length and n_{eff} is the effective index of the fiber core. When the grating is subject to a change in temperature, the shift of the Bragg wavelength can be obtained as

$$\Delta\lambda_{\mathrm{B}} = 2\Big(\Lambda\frac{\partial n_{\mathrm{eff}}}{\partial T} + n_{\mathrm{eff}}\frac{\partial \Lambda}{\partial T}\Big)\Delta T, \tag{2}$$

where T is the temperture. This fractional wavelength shift may also be written as

$$\Delta\lambda_{\mathrm{B}} = \lambda_{\mathrm{B}}(\alpha + \xi)\Delta T, \tag{3}$$

where $\alpha = (1/\Lambda)(\partial\Lambda/\partial T)$ is the thermal expansion coefficient of the fiber and $\xi = (1/n)(\partial n/\partial T)$ is the thermo-optic coefficient. Equations (2) and (3) both show that the thermally induced wavelength shift has two major contributions: the changes in the length of the grating period and in the effective index of the fiber. For a POF

Bragg grating, the thermal expansion coefficient α can reach 10^{-5} order, while the thermo-optic coefficient ξ is typically equal to -10^{-4} order[18]. The accuracy parameters depend on the variety of the materials comprising the POF. Figure 1 shows the simulation of temperature response of a POF Bragg grating in contrast to silica optical FBG, which is well known to be $\alpha = 0.55 \times 10^{-6}$ and $\xi = 6.3 \times 10^{-6}$, assuming that the Bragg wavelength λ_B is 1550 nm at 20 °C. This can be represented mathematically as

$$\lambda_B = 1550(1 - 9 \times 10^{-5}T). \qquad (4)$$

The slope of this curve is negative, indicating that the Bragg wavelength will decline as the temperature rises due to the negative bulk thermo-optic coefficient. The changes in the effective index and thermal expansion would enable the Bragg wavelength to move contradirectionally as temperature changes. The thermo-optic coefficient is one order of magnitude higher than the thermal expansion coefficient, leading to the suppression of thermal expansion. The Bragg wavelength of silica optical FBG can be represented as

$$\lambda_B = 1550(1 + 6.85 \times 10^{-6}T). \qquad (5)$$

Differently, this slope is positive and both the factors make the Bragg wavelength shift toward the same direction. The slope of POF Bragg grating is much bigger than that of silica optical FBG, which means that it is more sensitive to changes in temperature.

The POF preform is made using the Teflon technique[19]. The cladding is made of MMA-ethylmeth acrylate (EMA), and the core is made of MMA-EMA-benzoylm-ethacrylate (BzMA) + 2 wt.-% BDK. The refractive index difference between the core and cladding is about 0.001. The BDK was introduced to the core as the photosensitive doping material, which is a classic photosensitive dye that exhibits photodegradable character under a very wide band of ultraviolet (UV) illumination. The refractive index change caused by this process is estimated to be 4.5×10^{-5}. The BzMA was used to adjust the refractive index of the core. The preform was then heat-drawn into a POF by taking up spool at fixed drawing velocity and temperature. The diameters of the core and the cladding are 11 and $230\,\mu m$, respectively. We selected a 20-cm-long part of the POF, which is consistent with the fiber drawing process for inscribing Bragg grating. The POF was operated in single mode near 1570 nm.
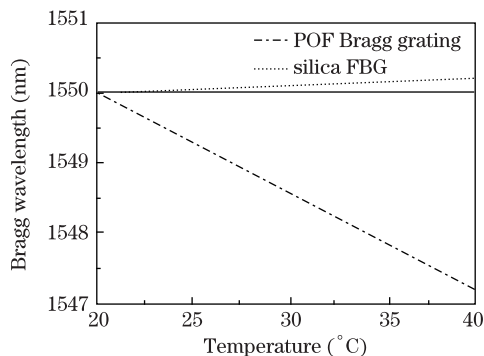
The Bragg grating was fabricated by the irradiation of the interference fringes formed by the two-beam interference method. The experimental setup is shown in Fig. 2. The POF was placed on the top of the phase mask. A 355-nm frequency-tripled Nd:YAG pulse laser was used, and the period of the phase mask was 1061.4 nm. A modified sagnac optical ring interference system was set up to make only the two first-order beams diffracted by the phase mask involved in the interference while blocking the zero-order diffraction beam[20]. The two beams counter-propagated over the systems through three prisms will have nearly the same optical path in order to maintain the high visibility of interference fringes. The average power intensity for writing gratings is about 673 mW/cm². After 16 min of exposure, the Bragg grating was formed in the POF.

Figure 3 shows the configuration used to measure the character of the POF Bragg grating and its temperature response. The POF Bragg grating was connected to a 3-dB coupler, which enabled the reflected light from the grating to be directed to the optical spectrum analyzer (AQ6317C, Agilent). We used the space coupling method to make the POF coupled with a single-mode silica fiber; thus, the splicing loss and reflection power would also be dependent on the coupling efficiency between the silica fiber and the POF. An incubator was used as the heat setup, whose temperature was controlled automatically. The accuracy of temperature measurement is 0.1 °C and needs several minutes to be stable at the desired temperature. Figure 4 shows the reflection spectra of the POF Bragg grating under three different temperatures. The full-width at half-maximum (FWHM) of the reflection peak was 0.3 nm. The reflection power was 5–8 dB above the noise level. A potential method to improve the efficiency of POF Bragg grating is reducing the writing power and increasing the length of the grating period. In addition, we need to find a critical time for the writing in order to obtain the largest reflection power. From the spectrum, it can be seen that the reflection amplitude peak of the POF Bragg grating shows large fluctuation with temperature change. This was mainly due to the replacement at the joining of the silica fiber and the POF inside the connector. The silica fiber and the POF have different thermal expansion as temperature changes, leading to the variation of coupling efficiency. One possible way to avoid this fluctuation is to make only the grating part

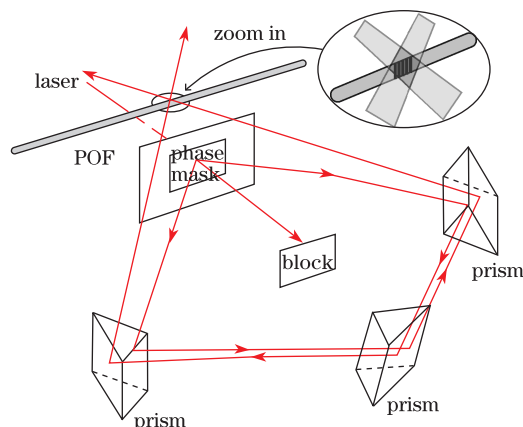Fig. 1. Simulation of temperature response of POF Bragg grating and silica optical FBG.

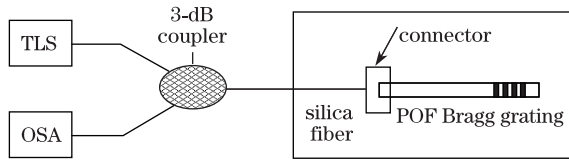Fig. 2. Configuration used to write grating in POF.

Fig. 3. Configuration used to measure the temperature response of POF Bragg grating. TLS: tunable laser source; OSA: optical spectrum analyzer.
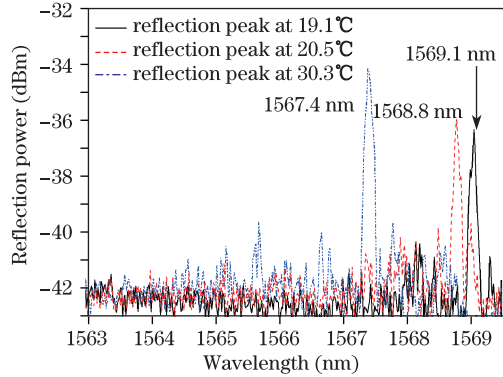

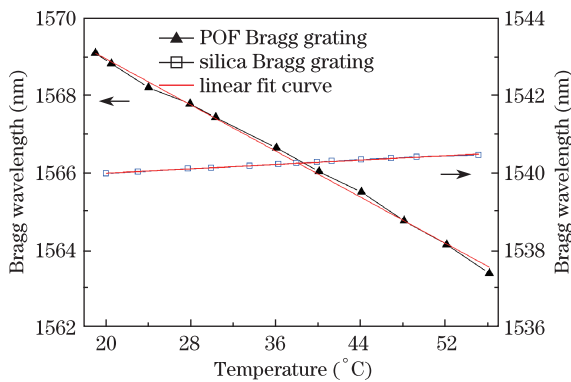Fig. 4. Reflection spectra of POF Bragg grating at different temperatures.

Fig. 5. Temperature response of POF Bragg grating and silica optical FBG.

of the POF in the temperature change area. The temperature response characters of the POF grating and silica optical FBG are measured and shown in Fig. 5.

The measurement is from 20 to 60 °C. The Bragg wavelength of the POF Bragg grating decreased, while the silica optical FBG rose with the increase of temperature. The reproducibility of the response to temperature is well over repeat measurements, and the result is in good agreement with the theory calculation. The result shows that the two temperature response curves are relatively linear. The expressions of the two curves are

$$\lambda_{\mathrm{B}} = 1571.916 - 0.149T (\text{POF Bragg grating}), \quad (6)$$

$$\lambda_{\mathrm{B}} = 1539.677 + 0.0141T (\text{silica optical FBG}). \quad (7)$$

This indicates that the temperature sensitivity of POF Bragg grating is 149 pm/°C, while that of the silica optical FBG is 14.1 pm/°C.

In conclusion, a single-mode POF with a highly photosensitive core doped with BDK is fabricated and used for writing POF Bragg grating. The temperature sensitivity of the single-mode POF Bragg grating is found to be 149 pm/°C. This character makes the POF grating appear to be very attractive for constructing temperature sensors with high sensitivity.

References

1. A. D. Kersey, M. A. Davis, H. J. Patrcik, M. LeBlanc, K. P. Koo, C. G. Askins, M. A. Putnam, and E. J. Friebele, J. Lightwave Technol. **15,** 1442 (1997).
2. J. Jung, H. Nam, B. Lee, J. O. Byun, and N. S. Kim, Appl. Opt. **38,** 2752 (1999).
3. M. G. Xu, L. Dong, L. Reekie, J. A. Tucknott, and J. L. Cruz, Electron. Lett. **31,** 823 (1995).
4. M. G. Xu, L. Reekie, Y. T. Chow, and J. P. Dakin, Electron. Lett. **29,** 398 (1993).
5. Y. X. Jin, C. C. Chan, X. Y. Dong, and Y. F. Zhang, Opt. Commun. **282,** 3905 (2009).
6. H. Zhao, J. Bao, and Y. Chen, Acta Opt. Sin. (in Chinese) **28,** 1681 (2008).
7. Y. Miao, B. Liu, and Q. Zhao, Acta Opt. Sin. (in Chinese) **28,** 2072 (2008).
8. T. L. Yeo, T. Sun, K. T. V. Grattan, D. Parry, R. Lade, and B. D. Powell, IEEE Sensors Journal **5,** 1082 (2005).
9. Y.-Q. Liu, Z.-Y. Guo, Z.-G. Liu, D.-H. Zhao, C.-F. Ge, and X.-Y. Dong, Chin. Phys. Lett. **17,** 115 (2000).
10. W.-G. Jung, S.-W. Kim, K.-T. Kim, E.-S. Kim, and S.-W. Kan, IEEE Photon. Technol. Lett. **13,** 1209 (2001).
11. G. D. Peng, Z. Xiong, and P. L. Chu, Opt. Fiber Technol. **5,** 242 (1999).
12. Z. Xiong, G. D. Peng, B. Wu, and P. L. Chu, IEEE Photon. Technol. Lett. **11,** 352 (1999).
13. M. P. Hiscocks, M. A. van Eijkelenborg, A. Argyros, and M. C. J. Large, Opt. Express **14,** 4644 (2006).
14. J. M. Yu, X. M. Tao, and H. Y. Tam, Opt. Lett. **29,** 156 (2004).
15. P. J. Scully, D. Jones, and D. A. Jaroszynski, J. Opt. A: Pure Appl. Opt. **5,** S92 (2003).
16. H. B. Liu, H. Y. Liu, G. D. Peng, and P. L. Chu, Opt. Commun. **219,** 139 (2003).
17. H. F. Taylor, *Fiber Optic Sensors* F. T. S. Yu and S. Yin, (eds.) (Dekker, New York, 2002) Chaps. 2 and 4.
18. J. M. Cariou, J. Dugas, L. Martin, and P. Michel, Appl. Opt. **25,** 334 (1986).
19. G. D. Peng, P. L. Chu, Z. Xiong, T. W. Whitbread, and R. P. Chaplin, J. Lightwave Technol. **14,** 2215 (1996).
20. Z. Xiong, G. D. Peng, B. Wu, and P. L. Chu, J. Lightwave Technol. **17,** 2361 (1999).